

Flow Characteristics of the HANARO Reactor Pool

Heonil Kim¹ and Gee Yang Han
Korea Atomic Energy Research Institute
P.O.Box 105, Yuseong
Daejeon, 305-600, Korea
Tel: Int+8242-8688490
Email: hkim@kaeri.re.kr

ABSTRACT

HANARO is an open-tank-in-pool type research reactor. Out of the returning PCS (Primary Cooling System) flow, about 10% flow is directed to the bottom of the reactor pool (90% flow to the core). The flow inside the reactor pool due to this bypass flow is analyzed by a commercial computational fluid dynamics code, CFX-4. The change of the flow pattern inside the reactor pool is also studied including hot water layer (HWL) in the case where hotter bypass flow than the pool is dumped.

A. General

HANARO reactor pool is cylindrical and its size is 4m in diameter and 12.2m in depth. It houses reactor structures including a reactor core, inlet and outlet pipes, a chimney, and a reflector tank at the bottom. Ten percent of the total flow is fed into the bottom of the pool and thus the same amount of pool water is being sucked through the chimney opening; this is called the bypass flow. This bypass flow merges to the core flow inside the chimney and then exits through the two outlet nozzles attached at the side of the chimney wall. At the top of the reactor pool, a hot water layer is formed. This prevents activated reactor pool water from reaching to the top of the pool surface by buoyant force, where workers are present. This report summarizes the simulation of how the bypass flow behaves and the hot water layer is affected.

The bypass flow is flowing down through a 6inch pipe. At the elevation of 73.98, part of the flow goes to the grid plate cooling header just below the grid plate. At the elevation 72.5m (0.2m above the pool bottom) the remainder ejects into the pool horizontally, both in the northeast and the northwest direction. For calculational purpose, 30% of bypass flow is assumed to go to the cooling header and the rest 70% to the pool, where the northeast flow is assumed to be 150% of the northwest flow by considering the flow resistance of the two horizontal pipes.

In real operation, the HWL is formed before powering up the reactor, hence the simulation follows this. In the calculation of the pool behavior, a HWL is formed by circulating 50°C water for 2 hours and then the bypass flow is dumped into the pool. When the bypass flow temperature is the same as the pool water, the flow inside the pool reaches a steady state at 1500sec, which is believed to be a final solution. The case of hotter bypass flow than pool is also studied to see the effect of the bypass flow on the HWL.

B. Calculation Method

¹ Heonil Kim, Korea Atomic Energy Research Institute, P.O.Box 105, Yuseong, Daejeon, Korea

(1) Mesh Modeling

Since the calculation domain is the reactor pool, the reactor structures including the inlet plenum, intermediate column shell, reflector tank surrounding the core are modeled as cylinders with appropriate size. The space between those cylinders and the pool liner are turned into the calculation space. Inlet and outlet pipes are all neglected.(Fig .1)

A 30% bypass flow is assumed to feed from the intermediate column shell under the reflector tank into the pool horizontally in 4 directions. The rest 70% flow is fed from two pipes at the vicinity of the south pool liner, whose direction is northeast and northwest. Its direction and the magnitude are treated as boundary conditions using inlet patch option in the CFX-4. The hot water from the HWL heater system is assumed to enter the north pool using a boundary condition. The exit lies 244 degrees in a counterclockwise direction from the entering location seen from the top of the pool. In the calculation, the exit locates at 252 degrees due to the limitation of the modeling. Figure 2 shows the inlet and outlet location of the HWL system. The size of the inlet and outlet for the HWL had to be modeled bigger than reality for better convergence. The flow rate of HWL and bypass (1.44kg/s and 77kg/s) were adjusted using boundary conditions. Meshes were produced such that the differences in cell size to the neighboring cell are as small as possible. The number of meshes used in this calculation is 28620.

(2) Assumptions

The following assumptions are made in the calculation.

- ① Neglect service pool, canal, and PCS pipes.
- ② Laminar Flow.
- ③ Transient.
- ④ Insulated Walls.
- ⑤ Consider natural convection.

C. Results and Discussions

Since the two horizontal bypass pipes are not symmetrically connected to the main bypass line, the bypass flow rate must be different due to the flow resistance. The main interests lie in the analysis of flow characteristics due to this different flow injection. Hand calculated mass flow ratio for the northeast and the northwest was 1.5 : 1 and these values were input by varying the x and z components of the velocities. A trial and error method was applied to match the calculated bypass flow rate equal to the real value, 77kg/s.

Initially adaptive time step was tried but it did not converge well. Therefore, 40 seconds of fixed time step (time step 0.2s) calculation was done and then the adaptive time step calculation was resumed using the fixed time step calculation results as the initial conditions, which resulted in a converged solution. The residuals for u-, v-, w-momentum, mass source, energy were larger than 1.6×10^3 which meant a good convergence. To get rid of possible unstable convergence the under-relaxation factor of 0.4 for each variable was used throughout the whole calculations.

During the adaptive time step calculation all residuals for each velocity component, enthalpy, etc. were found to converge well for each time step. The convergence test for this problem was done on u-velocity. In order to achieve a stable calculation, a minimum of 7 iterations were forced to be executed before transferring to the next time step even when the convergence test was satisfied. A maximum time step was determined for stable and efficient calculation.

The location and size for the inlet and outlet of the HWL system were arbitrarily selected but it would not affect the whole pool water distribution, hence it is acceptable: the increase of inlet and outlet opening size and the change of 8 degrees for the outlet were inevitable choices in order not to increase the required number of cells too much, determined by the

code. To simulate the formation of HWL, hot water of 50°C was assumed to circulate at the rate of 1.4kg/s for 2 hours which resulted in a HWL of 43°C at the pool top. When we calculate the pool behavior by bypass flow, the flow of the HWL system was assumed to cease. This was done for better convergence by making the problem simple. This assumption was later checked by introducing the HWL flow. The effect of the HWL flow on the whole reactor pool turned out to be trivial : the temperature of the HWL changed little during the entire calculation time (1500s) for the current bypass flow problem.

Figure 3 shows the flow pattern at the north-south-cut plane ($z=0$ plane). This is the result at 1500s after the bypass flow enters the pool. To show the incoming bypass flow, the flow pattern at the $y=0.2$ plane is overlapped in the same Figure. The bypass flow enters the pool both in the northeast and the northwest direction from the bottom south side of the reactor pool (in the Figure, left is the north and right is the south). The difference in the incoming flow rates seems to induce an asymmetric flow in the entire pool. In the bottom of the pool, relatively large velocity flow compared to other part of the pool is induced at the north side of the pool(bottom left of the Figure). In the middle of the pool, relatively large velocity flow is induced at the south side of the pool(middle right of the Figure). Since the bypass flow enters the pool, the same amount of pool water should be sucked away. In the figure, some pool water is seen to go down through the top opening of the chimney.

Figure 4 shows the flow pattern at the north-south-cut planes, $z=1.3$ and -1.3 planes. Left Figure($z=1.3$ plane) depicts the flow in the west pool where most of the flow is directed to the right. Right Figure($z=-1.3$ plane) contains the left direction flow. If one looks down the pool from the pool top, there exists a counterclockwise flow in the entire reactor pool. This is believed to occur due to the method of the bypass flow injection. The bypass flow enters the south pool in the northeast and the northwest direction. Those two incoming flows meet at the north side of the pool and direct up resulting in a counterclockwise revolving motion. The location of uprising flow inclined toward the west because the bypass flow velocity in the northeast direction is bigger, which can be seen in the bottom left Figure. The overall revolving motion in the pool can also be seen in the flow distribution on the horizontal planes shown next.

The flow distribution on the horizontal planes, 0.2, 1, 2, 3, 4, 5, 6, 7m from the pool bottom are shown in Figure 5. At 0.2m from the bottom, bypass flow is entering the pool in two directions. In most parts of the pool, counterclockwise revolving flow seen from the top is present. This is believed to occur because of the different incoming bypass flows. This revolving motion seems to have a bad effect on the pool water being sucked through the chimney top opening because it does not seem to be easy to suck this revolving pool water. If this revolving flow is present as in the simulation, there is a chance for this bypass flow to mix with HWL at the top of the pool.

Figure 6 shows the iso-surface of $v=0.1\text{m/s}$. In the Figure, X axis position indicates the pool south, where the bypass flow is injecting both in the northeast and the northwest direction. The figure shows the incoming bypass flow propagating along the pool liner, uprising flow starting to revolve counterclockwise and pool water going down through the chimney opening.

If the solution is correct, the pool water distribution should be the same even when we change the mesh sizes. Therefore, the calculation was repeated with decreased number of cells. The cell number was reduced to 17620, which is 62% of the previous calculation. Figure 7 shows the temperature and velocity distribution on $z=0$ plane for the cases of two different cell numbers. The two calculations show the same results which ascertains that the solution is well converged regardless of the cell numbers.

If the temperature of the bypass flow is large, it may rise up due to natural convection and may affect the HWL at the pool top. The calculation for this case was performed to analyze the flow behavior. The initial conditions are the same except that the temperature of the bypass flow is larger than that of the pool by 5°C . Figure 8 shows the temperature and velocity field at $t=120\text{s}$ and 300s after entering the hot bypass flow. In case of the same bypass temperature as that of the pool (right figure), the HWL maintains well and it

shows nearly the same result as in the result at 1500s(Figure 7). While, in the case of hotter bypass flow (left Figure), some upward motion is clearly seen in the bottom right of the HWL at the same time(120s). As a result, the bottom right of the HWL starts to collapse. At $t=300s$ the overall pool temperature is starting to change because of the mixing of hotter bypass flow and the colder pool water. This tells us that the temperature of the bypass flow should not be higher than that of the pool to guarantee the stable operation of the HWL system. And the thicker the HWL is the less the chance of collapse of the HWL. As a design application, the upgrade of the power of the HWL system was conducted since the initial operation was completed successfully.

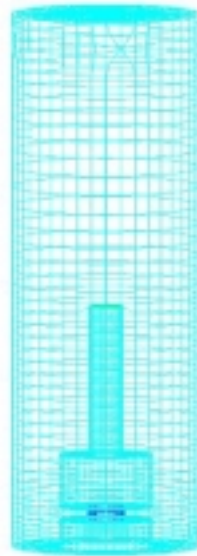


Figure 1. Calculation Domain for Reactor Pool

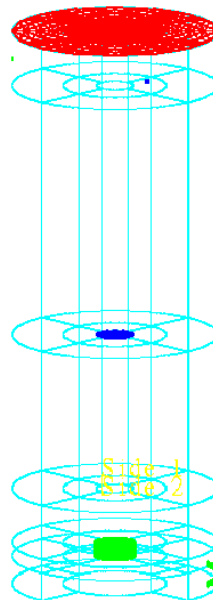


Figure 2. Inlet and Outlet Patch Model

- Red : Air-Water Interface (slip)
- Light Green : Inlet
- Blue : Exit

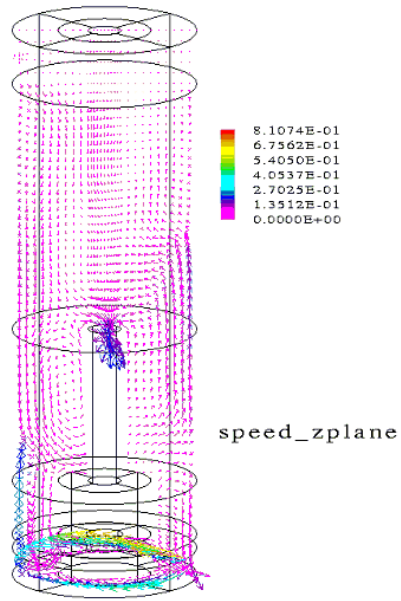


Figure 3. Flow Distribution at $z=0$ plane

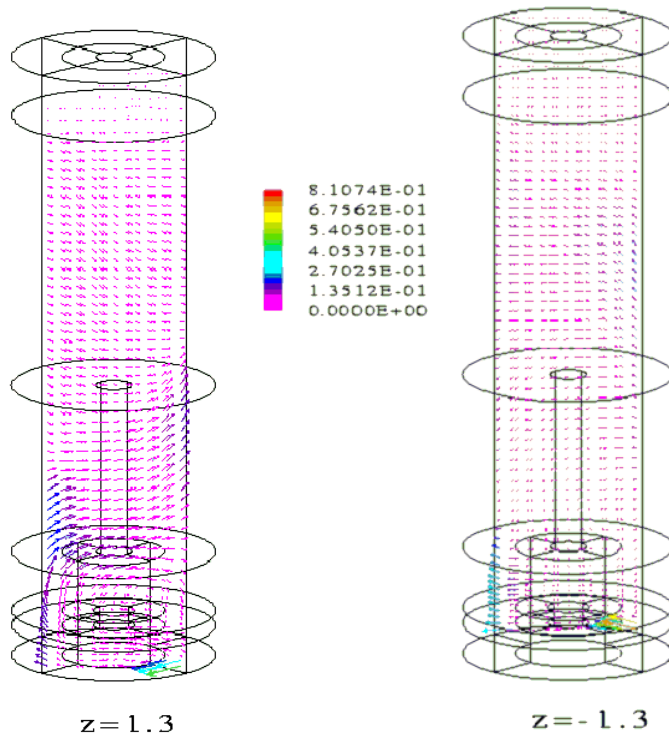


Figure 4. Flow Distribution at $z=1.3$ & -1.3 plane

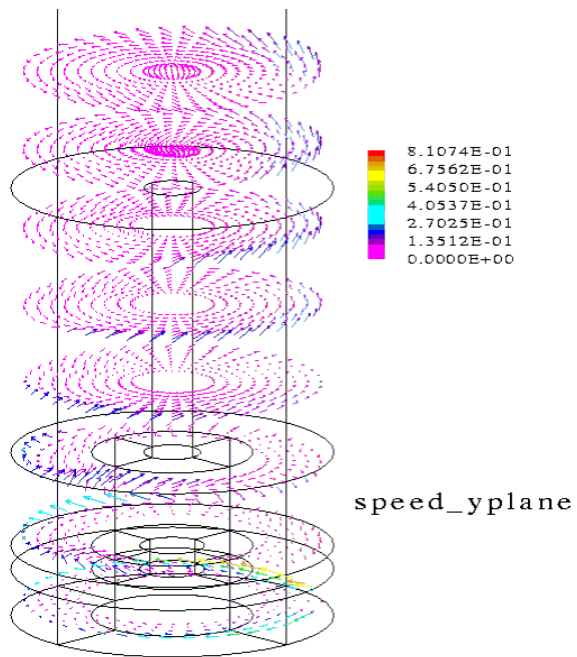


Figure 5. Flow Distribution at the Pool Bottom

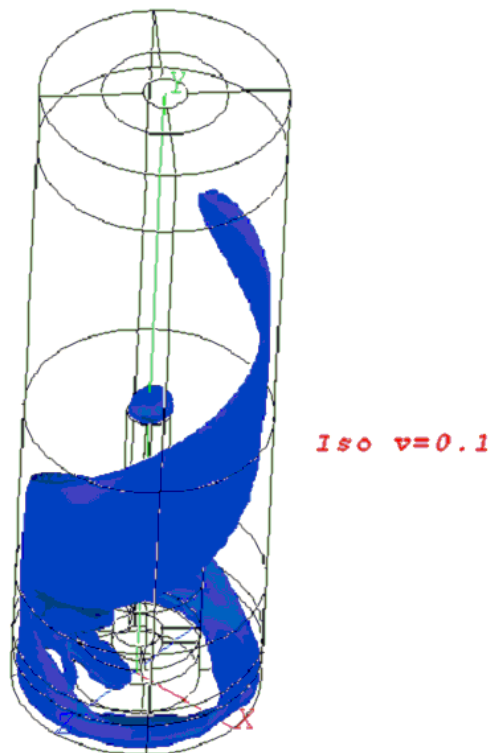
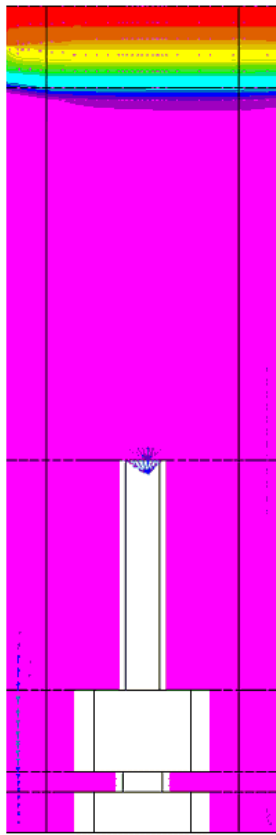


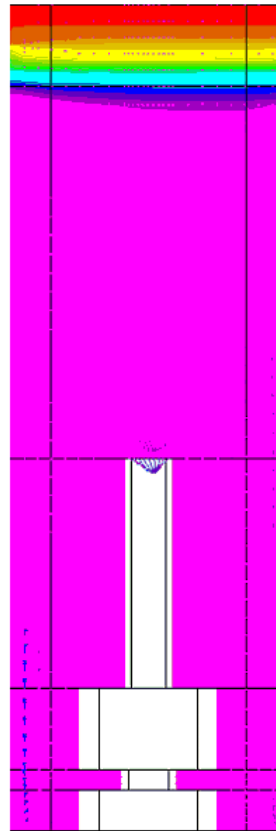
Figure 6. Iso-surface (v=0.1)



3.1577E+02
 3.1447E+02
 3.1318E+02
 3.1188E+02
 3.1059E+02
 3.0929E+02
 3.0800E+02

RxPool

cell number = 28620



3.1573E+02
 3.1444E+02
 3.1315E+02
 3.1187E+02
 3.1058E+02
 3.0929E+02
 3.0800E+02

RxPool_sm

cell number = 17620

Figure 7. Temperature & Flow Distribution (z=0 plane)

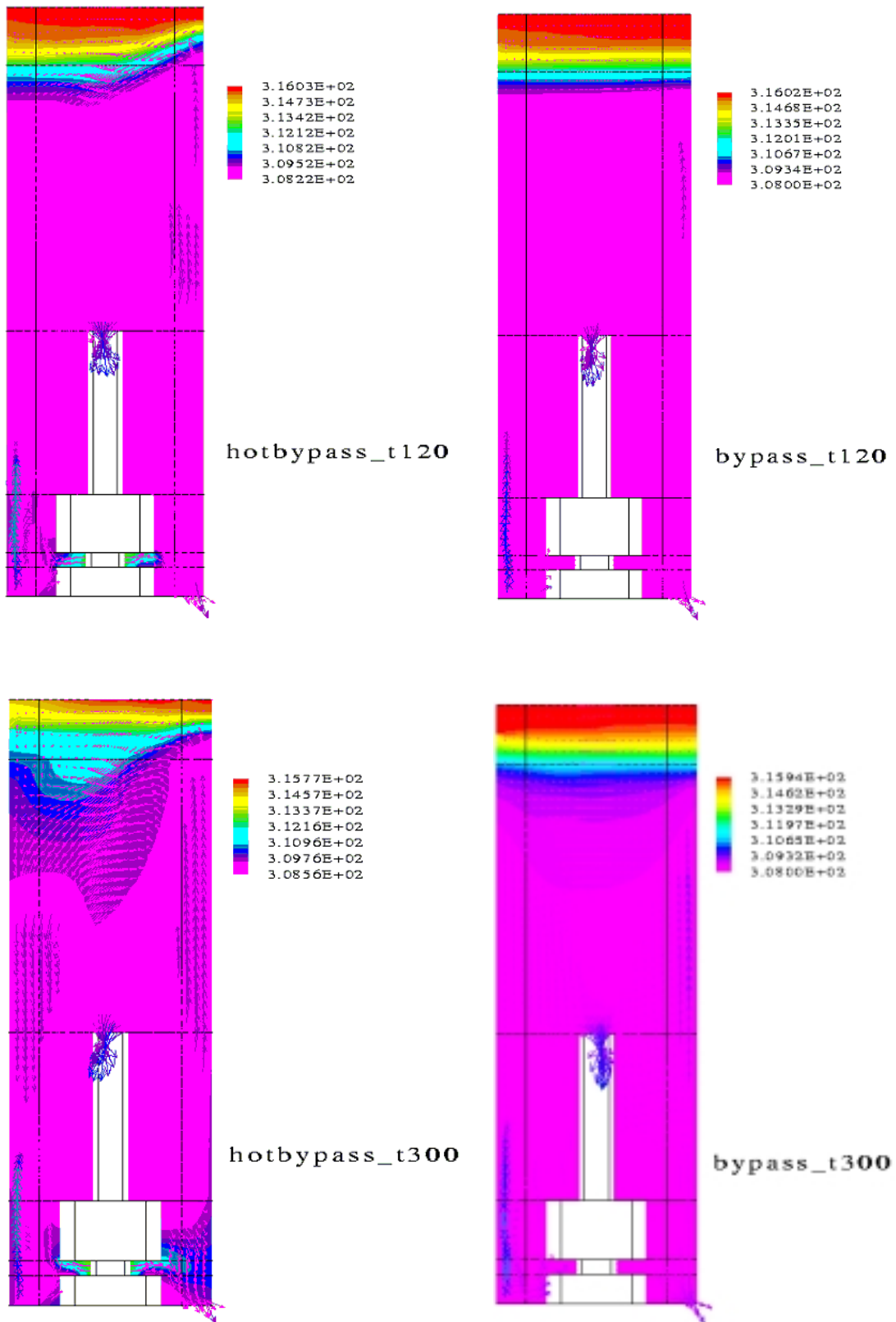


Figure 8. Temperature Change of Pool Due to Bypass Flow